JOURNAL OF PROPULSION AND POWER
Vol. 27, No. 2, March–April 2011

Reaction Dynamics of Aluminum-Viton®-Acetone Droplets

Sanjana Datta,* Birce Dikici,* Michelle L. Pantoya,† and Stephen Ekwaro-Osire†
Texas Tech University, Lubbock, Texas 79424

DOI: 10.2514/1.50408

The fluoroelastomer Viton ($C_5H_{3.5}F_{6.5}$) is a binder used in energetic material composites that can be dissolved in acetone and mixed with solid metal fuel particles, such as aluminum. The slurry can be molded into any configuration and the acetone is evaporated off leaving a solid homogeneous reactant mixture. Fundamentally understanding the reaction dynamics of acetone, Viton, and aluminum is useful for not only consolidating reactants, but also for the potential to use nanometric aluminum particles in liquid combustion applications. The objective of this study is to examine acetone-Viton droplet burning as a function of aluminum particle size and concentration. A diagnostic was developed that suspends the multiphase 3 mm droplet on a fiber and enables droplet surface regression rates to be monitored with a high-speed video camera. Results show that acetone combined with Viton (5%) and either 2.5% micron aluminum (10–14 μm) or nanometric aluminum (80 nm) burned with two distinct stages. However, acetone combined with Viton and more than 5% nanometric aluminum burned with a distinct three-stage behavior. The three stages are described as evaporation, combustion, and burning of carbon residue. Addition of micron aluminum to Viton and acetone droplets decrease the droplet regression rate 82% when compared with Viton and acetone droplets with nanometric aluminum particles. These results suggest that the presence of nanometric aluminum particles generates localized hot spots that consume the carbon present from Viton decomposition, thereby eliminating the third stage.

I. Introduction

NANOMETRIC particle fuels such as aluminum (Al) demonstrate unique combustion behaviors over their micron scale counterparts. When nanometric Al is combined with a metal oxide or organic or inorganic oxidizer the mixture may be referred to as a nano energetic material (nEM). These nEMs show dramatically increased burn rates [1] and reduced ignition times [2] over micron particle formulations. Several attempts to explain these behaviors have been reported in the literature [3–6].

One theory referred to as the *melt dispersion mechanism* has been newly introduced as a reaction mechanism based on mechanochemistry principles [5,6]. The mechanism describes the interaction between a pristine, high-melting temperature alumina shell and the lower-melting temperature aluminum (i.e., Al) core. At high heating rates, the Al core melts and expands exerting pressure on the alumina shell. The shell eventually ruptures by spallating such that unbalanced pressure waves cavitate the molten Al creating a dispersion of liquid Al droplets, which readily oxidize [5,6]. While no experimental evidence validates this proposed theory on a single particle scale, many macroscopic combustion behaviors have been observed that are consistent with this theory [7].

Macroscopic observations only appear consistent with the melt dispersion mechanism when Al nanoparticle shells have not been mechanically altered. For example, compressing the powders into pellets [8] or purposely grinding powders introduces imperfections in the oxide shell which reduce the shell strength under the high pressure load associated with Al core melting. In this way, these imperfections would inactivate the melt dispersion mechanism. A key assumption in the melt dispersion mechanism is that the alumina shell is virtually defect free such that its strength approaches the theoretical maximum [5].

One motivation for this study is to engineer an approach to consolidating powders such that mechanical imperfections to the alumina shell are not introduced. The approach would require the introduction of a liquid to produce a slurry that could be molded into a shaped charge as opposed to pressed. Liquid can be evaporated leaving a consolidated solid particle matrix. In this way, consolidated mixtures could potentially react according to the melt dispersion mechanism such that heightened reactivity may be better exploited.

There are many applications in which consolidating formulations by pressing and mechanically compacting powders is difficult. For example, a relatively new application for nEMs involves their integration into microelectro-mechanical (MEM) devices [9] where nEMs are used as actuators and/or initiators. One of the biggest challenges incorporating nEMs into MEM applications is depositing the nEMs into microchannel configurations. Some approaches involve tedious and expensive single molecule placement techniques [10]. These approaches may be difficult and costly to implement on a large scale. However, deposition of liquid-based slurry of nanoparticle reactants may be a viable approach offering lower cost and large scale-up potential as advantages.

Motivated by both the exploitation of the melt dispersion mechanism and MEM applications, the purpose of this study was to experimentally examine the fundamental reaction dynamics of a liquid droplet containing a reactive material formulation that includes nanometric Al particles (nm Al). This understanding is effectively a precursor to future efforts devoted to engineering a consolidated reactive material created via a slurry and mold-cast into a shape charge. This fundamental understanding is especially useful in safety protocols where accidental ignition can occur during the consolidation of the reactive material. In this way, understanding the burning behavior of the multiphase and multicomponent system better predicts the response for autoignition and accident scenarios associated with nEM consolidation.

To achieve this goal several oxidizers were examined for their solubility in a liquid medium. Viton®[‡] is a binder that has been used with Al [11] and was found here to dissolve in acetone. Viton ($C_5H_{3.5}F_{6.5}$) is a fluoroelastomer in which fluorine acts as an oxidizer. Fluorine is the most electronegative element and readily gains electrons. The Viton-acetone liquid mixture can be combined with Al particles to effectively coat Al particles with Viton after the evaporation of acetone. Hence, in the liquid-solid state, this mixture can be molded into any configuration before acetone evaporation. The introduction of this new mold casting consolidation approach

Received 19 April 2010; revision received 27 September 2010; accepted for publication 8 October 2010.

*Graduate Student, Mechanical Engineering Department.
†Professor, Mechanical Engineering Department.

‡The trademark symbol will be omitted for brevity.

Table 1 Material specifications

Material	Particle size	Manufacturer	Purity	Form factor
Acetone	N/A	Mallinckrodt	99%	Liquid
Aluminum	80 nm	NovaCentrix	99%	Spherical
Aluminum	10–14 μm	Alfa Aesar	97.5%	Spherical
Viton	N/A	Dupont	A(Grade)	Sheet

using Viton dissolved in acetone presents potential for many applications involving consolidated nEM reaction in which the structural integrity of the particles have not been sacrificed.

Coating Al particles with a binder has been reported in several journals. For example, the application of the coating plays a positive role in propulsion systems by reducing the accumulation of slag and erosion of the structural member [12]. Spherical micron-sized Al particles combined with an organic binder have been used as a coating for austenitic steel [13]. This aluminized coating acts as a thermal barrier, which protects the blades and vanes of gas turbines from oxidation and corrosion [13] Other uses of binder passivated Al have been reported by Jouet et al. [14], who showed an enhancement in the rate of Al combustion by the replacing the oxide passivation layer with a fluoropolymer on Al particles. Their work showed that passivating Al nanoparticles with molecules containing oxidizer species such as, perfluorocarboxylic acid, resulted in energy that enhanced the detonation wave produced by explosive formations [14].

The goal of this study is to understand the combustion behavior Al particles when combined with Viton-acetone solution as a function of Al particle size and composition. A secondary motivation for this study was to develop a synthesis process which coats Al particles with a fluoroelastomer that may have implications for consolidating high bulk density nEM. This study is a unique contribution to the field of combustion because the reaction dynamics of a fluoroelastomer dissolved in an organic compound with nm and micron Al additives has not been investigated in the literature. Additionally, the study was conducted using an original droplet suspending apparatus that can suspend droplets of approximately 3 mm. The objectives of this study are to 1) create a diagnostic that can test single or multicomponent droplets, and 2) examine the combustion dynamics of droplets seeded with nano compared with micron aluminum (Al) particles.

II. Experimental Setup and Testing Procedure

Multicomponent droplet mixtures were prepared by mixing acetone with 5% mass Viton. Originally, Viton was cut into approximately 5 mm cubically shaped pieces, measured to the appropriate mass and placed in acetone to dissolve (e.g., dissolve time corresponded to roughly 1 day). This mixture is fuel rich with an equivalence ratio of 2.3. The nm Al particles (80 nm) are of spherical morphology with 80% active Al content (i.e., 20% is in the form of alumina (Al_2O_3), consistent with the passivation shell surrounding the Al core). The micron particles also have a spherical morphology with 97.5% active Al content (i.e., 2.5% is in the form of alumina (Al_2O_3), consistent with the passivation shell surrounding the Al core). The materials are summarized in Table 1. Aluminum particles were added to the Viton-acetone mixture and sonicated using a Misonix Sonicator 3000 which has been shown to break up agglomerates and improve mixture homogeneity.

The experimental setup is illustrated in Fig. 1. A Phantom IV (Vision Research, Wayne, NJ) high-speed digital camera was attached is a K2 Long-Distance Microscope (Infinity Photo-Optical Company, Boulder, CO) for higher magnification. A fiber optic light source (Cole Parmer® Illuminator, 41720 series) increased the contrast between the droplets and background for improved visualization. An acrylic plate with a Nichrome wire was positioned underneath the droplet and quartz fiber. The Nichrome wire was connected to the voltage source and droplets were ignited by supplying 3 volts of AC current to the wire with a variac voltage transformer.

Droplet evaporation and combustion were recorded with the high-speed camera which captured images at 100 frames per second. The data for droplet regression rate were obtained using the Vision Research image processing and analysis software compatible with the Phantom IV.

A 1-mm quartz fiber (with a cylindrical cross section) droplet suspending apparatus was developed to suspend an average 3-mm droplet (illustrated in Fig. 2). The droplets were suspended from the quartz fiber using a syringe with a needle that enabled greater control over the droplet size. The support fiber geometrically distorts the shape of the burning droplet from spherical to ellipsoidal. Struk et al. [15] report the different methods researchers typically present the equivalent diameter. In this study, only the D_{max} was measured and normalized based on the assumption that gravitational distortion affected all droplets in the same way. A conventional method to

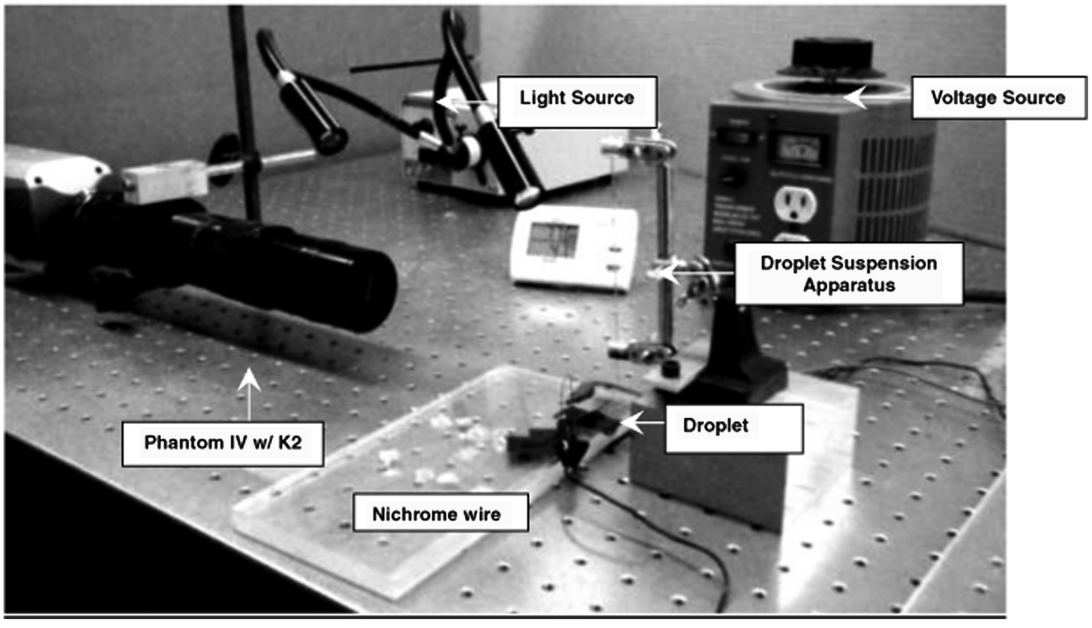

Fig. 1 Photograph of the experimental setup including droplet suspension apparatus, high-speed imaging camera and lens, light source, and nichrome wire ignition source.

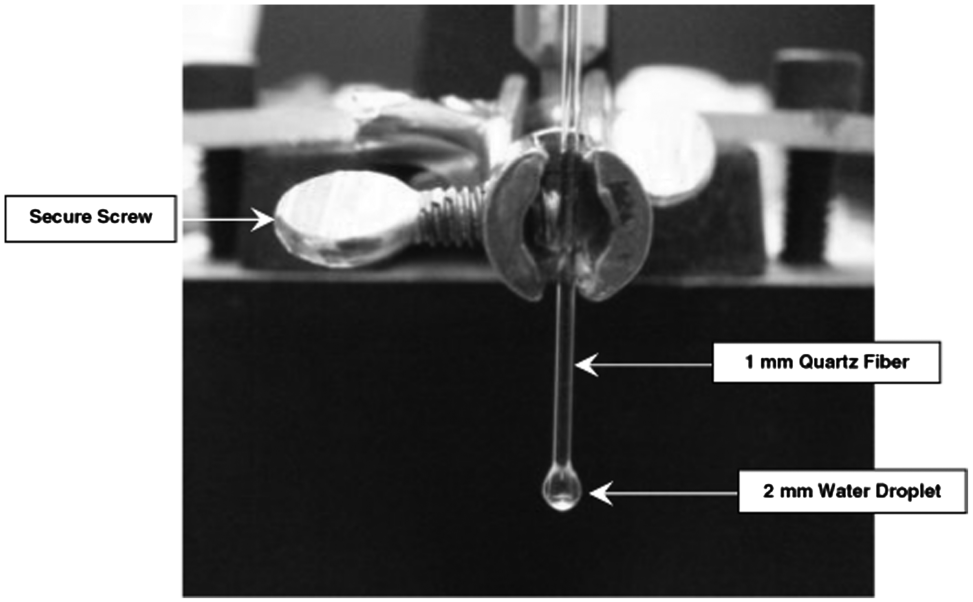

Fig. 2 Front view of the droplet apparatus with suspended water droplet for illustration purposes of size 2 mm diameter.

address the droplet diameter is the use of projected area (i.e., using both Dmax and Dmin, and assuming the droplet as an ellipsoid). It is noted that the regression rate using projected area was similar to the regression rate obtained with D_{max}, there was a 24% discrepancy. Since this study is a comparison of different compositions and the initial droplet diameters varied by approximately 1 mm, only Dmax was used in this analysis.

III. Results

Viton (5% by mass) burns with three distinct stages in an acetone droplet. The three stages are evaporation, combustion, and burning of carbon residue (Figs. 3 and 4). During the first stage, the droplet evaporates until it reaches an ignition threshold. The outer surface regression during evaporation is represented by a gentle slope at early times in Fig. 5a. The onset of combustion is distinguished in Fig. 5a by an inflection point in the droplet regression rate.

Figure 3 shows three consecutive still frame images during the transformation from evaporation to combustion for Viton-acetone droplets. These first two stages are also representative of those observed when Al particles are added to the droplet. The second stage begins with bubble formation inside the droplet and transitions to combustion (Fig. 3). Combustion appears uniform throughout the droplet and has a faster regression rate compared with the first stage:

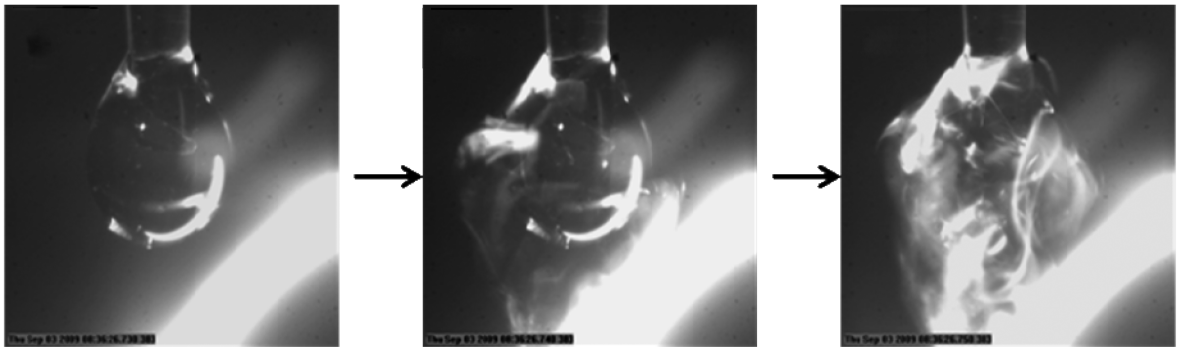

a) b) c)

Fig. 3 Still frame images of Viton-acetone droplet reaction dynamics: a) stage 1: evaporation; b) transition from evaporation to combustion; c) stage 2: combustion.

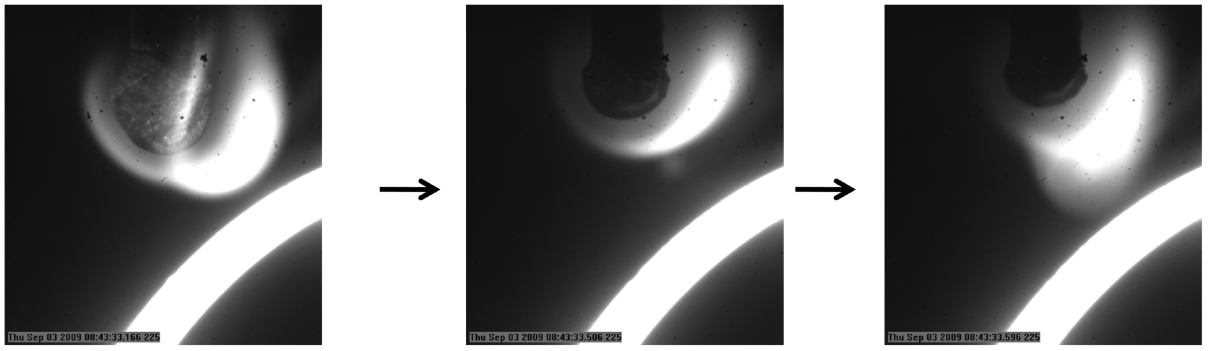

Fig. 4 Still frame images of third-stage combustion of carbon residue resulting from Viton-acetone droplet.

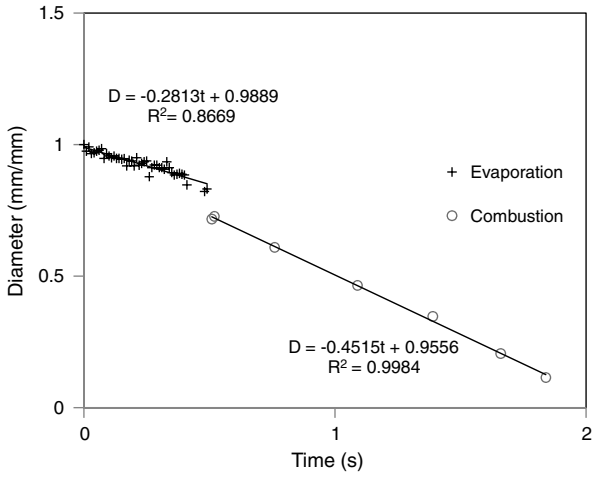

a)

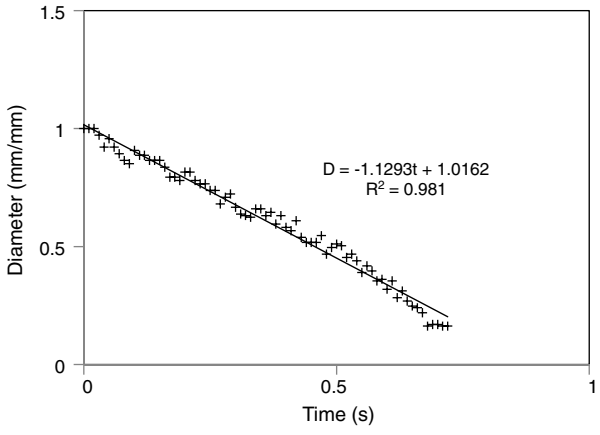

b)

Fig. 5 Viton-acetone droplet regression rate for a) stage 1: evaporation and stage 2: combustion; and, b) stage 3: combustion of carbon residue; time 0 corresponds to the beginning of third-stage combustion. Diameter presented on the axis was normalized by the initial droplet diameter.

evaporation (Fig. 5). Viton-acetone droplets also demonstrate a third stage which may correspond to combustion of remaining carbon with a distinct flame (Figs. 4 and 5b). The third stage is not observed when Al particles are added.

The second stage is determined by disruptive burning, the third stage is identified based on a distinct flame associated with burning of the solid residue. Also, an increase in burning rate is observed with transition from one stage to another (Fig. 5).

The bubble formation during stage 2 from within the liquid droplet and subsequent combustion can be described as *disruptive burning* and was observed to occur for the Viton-acetone droplets with and without the addition of Al particles. Disruptive burning can occur when one liquid in a multicomponent droplet reaches a nucleation temperature or when solid particles are added to a liquid droplet such that the interior of a droplet reaches a nucleation temperature, which results in interior vapor generation and consequent rapid disruption of the liquid [16]. During disruptive burning (stage 2), the rate of evaporation is negligible compared with the rate of combustion. For the Viton-acetone droplets Viton decomposes at 457°C and acetone boils at 56°C suggesting that initial disruptive burning may be triggered by boiling of acetone.

When Al particles are introduced the reaction dynamics are affected. With 2.5 mass % addition of micron or nm Al particles, the droplet takes on only a two-stage behavior (similar to that shown in Fig. 3). There was no burning of the excess carbon residue observed for these droplets. To investigate this further the second stage final

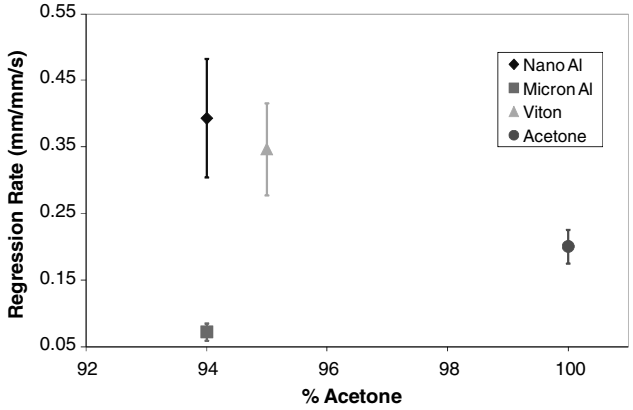

Fig. 6 Droplet regression rate comparison for acetone, Viton + acetone and nano-Al + Viton + acetone, and micron-Al + Viton+ acetone.

diameter for each sample was measured. The Viton-acetone droplet contains more carbon residue after the second stage compared with the nm-Al-Viton-acetone droplet. This second-stage final droplet diameter may be related to the ignition of the third-stage burning such that the third stage may be the result of unburned excess carbon.

As a baseline for comparison, pure acetone droplets were also observed. Figure 6 shows the addition of Viton and nm Al particles increases the regression rate of acetone. A third stage was not observed for the acetone droplets implying that excess carbon associated with Viton may be responsible for third stage burning in the Viton-acetone droplets. Figure 6 also shows the regression rate substantially reduces when micron Al particles are introduced. While there is not a significant regression rate deviation with addition of nm Al to the Viton-acetone droplets, there is a distinct change in burning behavior. Viton-acetone shows a three-stage burn behavior, whereas, 2.5 mass percent nm Al added to the Viton-acetone droplet only shows a two-stage behavior.

The mass percent of nm Al was doubled and then tripled to observe the difference in the regression rate and burn behavior. Figure 7 compares the regression rates of different percentages of nm Al. Even though no appreciable difference was observed in the regression rate, a third stage was observed with droplets having the highest concentration of Al. The third stage likely corresponds to burning of excess aluminum and was not similar to the third stage observed in Viton and acetone droplets in which that third stage corresponds with burning of excess carbon.

The regression rates shown in Figs. 6 and 7 are for stage 2: droplet combustion (excludes stage 1: evaporation). In this way, the burn time is measured from the onset of stage 2 to the end of reaction. The regression rates shown in Figs. 6 and 7 are normalized by the largest

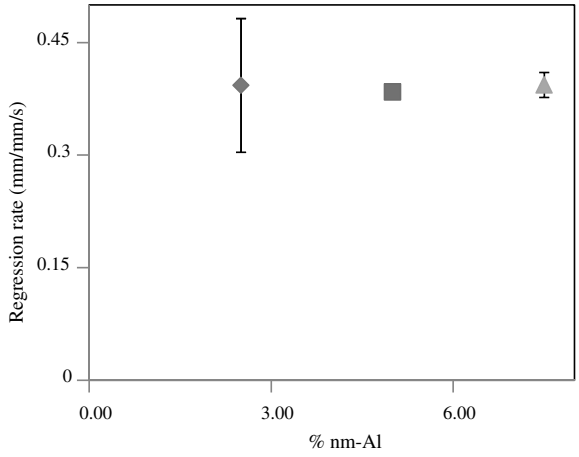

Fig. 7 Droplet regression rate comparison for different percentages of nm Al.

diameter (initial diameter of stage 2) and presented in terms of mm/mm/s. The normalized diameter was then plotted with respect to time and the slope of the line is the droplet regression rate presented on the y-axis of Figs. 6 and 7. The uncertainty associated with the measured droplet regression rates is limited by random measurement error based mainly on droplet position for the different tests. The standard deviation was estimated from the repeatability studies of each data set (five tests for each mixture composition).

IV. Discussion

One of the most interesting observations is the elimination of the third stage (burning of carbon residue) by the addition of Al to Viton-acetone droplets. The second stage final droplet diameter for Viton-acetone droplets was observed to be double the second stage droplet diameter for nm-Al-Viton-acetone droplet. This implies that the presence of Al may facilitate localized reaction sites that produce temperatures high enough to consume carbon from decomposing Viton. Osborne and Pantoya [17] showed that fluorine from polythetrafluoroethylene (Teflon) bonds with Al particles and facilitates Teflon decomposition at reduced temperatures. Further analysis revealed that fluorine actually bonds to vacant–OH sites on the surface of alumina (Al_2O_3) [18]. Aluminum particles are passivated with an alumina shell, and the specific surface area of the alumina shell has an effect on the onset of decomposition of the fluoropolymer (Teflon) [19]. As the specific surface area is increased, the onset of Teflon decomposition is reduced to lower temperatures [17,19]. In a similar way, fluorine from Viton may be attracted to Al particles and similarly catalyze the decomposition of Viton. The aluminum fluorination reaction (i.e., $Al + 3F \rightarrow AlF_3$) has an adiabatic flame temperature of 4352 K (computed using the thermal equilibrium program REAL (Tim Tech, LLC). The localized hot spots resulting from this reaction could also consume carbon thereby reducing the amount of carbon residue available for third-stage reaction. This may explain the elimination of the third-stage carbon residue burning in the Al-Viton-acetone droplets.

The characteristic time for thermal diffusion through an Al particle can be calculated as $\tau_{\text{diff}} = d_o^2/\alpha_{\text{Al}}$ where α_{Al} is a weighted average of the thermal diffusivity of the $Al + Al_2O_3$ composite particle and d_o is the initial particle diameter. For the nm Al particles τ_{diff} is 8×10^{-11} s and for the micron Al particles τ_{diff} is 1×10^{-6} s. This estimate shows that the characteristic time for heat to diffuse through the smaller particles is roughly 5 orders of magnitude faster than for the larger particles.

A chemical time scale (τ_{rxn}) for the reaction can also be estimated by the derivation of a chemical time scale for the rate limiting bimolecular reaction in Eq. (1). This rate limiting reaction is assumed based on the kinetic model for acetone oxidation which is assumed to be a rate limiting step in this reaction [20]. The following rate expressions are used in Eqs. (2) and (3)

$$\dot{\text{H}} + \text{O}_2 \rightarrow \dot{\text{O}} + \dot{\text{O}}\text{H} \tag{1}$$

$$\frac{\text{d[H]}}{\text{d}t} = -\kappa[\text{H}][\text{O}_2] \tag{2}$$

$$\frac{\text{d[O}_2\text{]}}{\text{d}t} = -\kappa[\text{H}][\text{O}_2] \tag{3}$$

If Eq. (3) is divided by Eqs. (2) and (4) is obtained

$$\frac{\text{d[O}_2\text{]}}{\text{d[H]}} = 1 \tag{4}$$

such that

$$[\text{O}_2] = [\text{H}] + c \tag{5}$$

where

$$\text{c} = [\text{O}_2]_0 - [\text{H}]_0 \tag{6}$$

and $[H]_0$ and $[O_2]_0$ are the initial concentrations of H and O_2 at the time $t = 0$.

Substituting Eq. (5) into Eq. (2) for $[O_2]$ and rearranging yields Eq. (7)

$$\int_{[\text{Al}]_0}^{[\text{Al}]} \frac{\text{d[H]}}{[\text{H}]([\text{H}] + c)} = -\int_0^t \kappa \, \text{d}t \tag{7}$$

Evaluating the integrals and setting $t = \tau_{rxn}$ when $[H] = [H]_0/e$ yields

$$\tau_{rxn} = \frac{1}{\kappa c} \ell_n \left(\frac{[\text{H}]_0 + ec}{[\text{H}]_0 + c} \right) \tag{8}$$

In the case where $[O_2]_0 = [H]_0$ such that $c = 0$, Eq. (6) does not directly apply. In this case, though, Eq. (8) can still be used by applying l'Hopital's rule for the limit $c \rightarrow 0$ and Eq. (8) simplifies to

$$\tau_{rxn} = \frac{e - 1}{\kappa[\text{H}]_0} \tag{9}$$

In Eq. (9) κ is the rate constant given by Eq. (10) [20] where T is the adiabatic flame temperature (3342 K)

$$\kappa = 3.547 \times 10^{15} T^{-0.406} \exp\left(-\frac{8359}{T} \right) \tag{10}$$

The initial concentration of H, $[H]_0$ can be calculated from

$$[\dot{\text{H}}]_0 = x_{\dot{\text{H}}} \frac{P}{R_u \bar{T}} \tag{11}$$

In the above equations, the reactants are assumed in equal proportions such that the mole fraction of H is assumed to be 0.5 (i.e., $x_{\dot{\text{H}}} = 0.5$). Additional assumptions are for 1 atm pressure and the universal gas constant is $R_u = 8315$ J/kmol K. The average temperature $\bar{T}$ is 322.5 K. From the above equations $\kappa = 10.7 \times 10^5$ m^3/(mol · sec), and $[H]_0 = 18.894$ mol/m^3, τ_{rxn} is 8.4×10^{-9} sec.

Based on these characteristic times, for the nanoparticles $\tau_{\text{diff}} < \tau_{rxn}$ such that nm Al particles are likely to more fully react to completion during acetone combustion while the micron Al particles may act as a heat sink because $\tau_{\text{diff}} > \tau_{rxn}$. For the micron Al particles this implies that the acetone reaction occurs faster than heat can fully diffuse through the larger particles such that only the surface of the micron Al particles may be participating in the combustion. The thermal lag associated with the micron Al particles may explain the significantly reduced regression rates depicted in Fig. 6.

In the recent literature, Gan and Qiao [21] examined the influence of nano and micron-sized Al particles burning in ethanol-based or n-decane-based liquid fuels. They found that for nano-Al particles, Brownian motion dominated the fluid movement and resulted in greater agglomeration of particles and a distinct final stage of burning associated with the Al agglomerated residue. For micron Al droplet suspensions, Brownian motion was least important and resulted in more complete combustion. A similar trend was observed in our study in that high concentrations of nano-Al resulted in third-stage Al residue burning, but this third stage was not observed when micron Al particles were used in place of nano-Al particles.

V. Conclusions

The reaction dynamics of multicomponent droplets were investigated. The droplets of acetone with the fluoroelastomer (Viton) demonstrate a three-stage behavior. The three stages are evaporation, combustion, and burning of excess carbon. When the droplets contain 2.5% mass of either micron or nm Al particles, localized hot spots generated from Al reaction may consume excess carbon, thereby eliminating the third stage. It was also determined that the regression rate for droplets with 2.5% micron Al decreases 82%

when compared with droplets with nm Al. The larger Al particles may act as a heat sink because their characteristic diffusion times exceed the assumed rate limiting acetone reaction time. Because there was no accelerated burn rate observed with the addition of nm Al, accidental ignition of Viton, acetone, and nm Al at the given compositions may require similar safety protocols as Viton mixed with acetone. When droplets contain 5% mass Al particles a third stage is observed, but likely corresponds to burning of Al rather than burning of excess carbon. There is a distinct difference in the appearance of the flame associated with carbon versus aluminum third stage burning. These results are consistent with the literature that shows Brownian motion associated with nano-Al particle suspensions results in greater agglomeration and a final stage associated with Al burning.

Dissolving Viton in acetone and adding Al is a technique that can be used to coat Al particles with a fluoroelastomer. Examining the combustion of the acetone-Viton-Al system has implications toward the safe handling of this energetic material synthesis technique.

References

[1] Bockmon, B. S., Pantoya, M. L., Son, S. F., Asay, B. W., and Mang, J. T., "Combustion Velocities and Propagation Mechanisms of Meta-Stable Intermolecular Composites," *Journal of Applied Physics*, Vol. 98, No. 6, 2005, p. 064903. doi:10.1063/1.2058175

[2] Granier, J. J., and Pantoya, M. L., "Laser Ignition of Nanocomposite Thermites," *Combustion and Flame*, Vol. 138, No. 4, 2004, pp. 373–383. doi:10.1016/j.combustflame.2004.05.006

[3] Rai, A., Zhou, L., Prakash, A., McCormick, A., and Zachariah, M. R., "Understanding and Tuning the Reactivity of Nano-Energetic Materials," *Materials Research Society Symposium Proceedings*, Vol. 896, Materials Research Society, Boston, 2006, pp. 99–110.

[4] Pantoya, M. L., and Granier, J. J., "Combustion Behavior of Highly Energetic Thermites: Nano Versus Micron Composites," *Propellants, Explosives, Pyrotechnics*, Vol. 30, No. 1, Feb. 2005, pp. 53–62.

[5] Levitas, V. I., Asay, B. W., Son, S. F., and Pantoya, M. L., "Melt Dispersion Mechanism for Fast Reaction of Nanothermites," *Applied Physics Letters*, Vol. 89, No. 7, 2006, p. 071909. doi:10.1063/1.2335362

[6] Levitas, V. I., Pantoya, M. L., and Dikici, B., "Melt Dispersion Versus Diffusive Oxidation Mechanism for Aluminum Nanoparticles: Critical Experiments and Controlling Parameters," *Applied Physics Letters*, Vol. 92, No. 1, 2008, p. 011921. doi:10.1063/1.2824392

[7] Watson, K. W., Pantoya, M. L., and Levitas, V. I., "Fast Reactions with Nano and Micron Aluminum: A Study on Oxidation Versus Fluorination," *Combustion and Flame*, Vol. 155, No. 4, 2008, pp. 619–634. doi:10.1016/j.combustflame.2008.06.003

[8] Pantoya, M. L., Levitas, V. I., Granier, J. J., and Henderson, J. B., "The Effect of Bulk Density on the Reaction Dynamics in Nano and Micron Particulate Thermites," *Journal of Propulsion and Power*, Vol. 25, No. 2, March–April 2009. doi:10.2514/1.36436

[9] Rossi, C., Zhang, K., Estève, D., Alphonse, P., Tailhades, P., and Vahlas, C., "Nanoenergetic Materials for MEMS: A Review," *Journal of Microelectromechanical Systems*, Vol. 16, No. 4, pp. 919–931.

[10] Menon, L., Bhargava Ram, K., Patibandla, S., Richter, C., and Sacco, A., Jr., "Ignition in Al-Fe2O3 Nanocomposites," *Materials Research Society Symposium Proceedings*, Vol. 901, Materials Research Society, Boston, 2005, pp. 140–143.

[11] Yarrington, C. D., Son, S. F., and Foley, T. J., "Combustion of Silicon/Teflon/Viton and Aluminum/Teflon/Viton Energetic Composites," *Journal of Propulsion and Power*, Vol. 26, No. 4, July–Aug. 2010, pp. 734–743. doi:10.2514/1.46182

[12] Glotov, O. G., Yagodnikov, D. A., Vorob'ev, V. S., Zarko, V. E., and Simonenko, V. N., "Ignition, Combustion, and Agglomeration of Encapsulated Aluminum Particles in a Composite Solid Propellant. II. Experimental Studies of Agglomeration," *Combustion, Explosion and Shock Waves*, Vol. 43, No. 3, May 2007, pp. 320–333. doi:10.1007/s10573-007-0045-y

[13] Kolarik, V., Juez-Lorenzo, M., Anchústegui, M., and Fietzek, H., "Multifunction High Temperature Coating System Based on Aluminium Particle Technology," *Materials Science Forum*, Vols. 595–598, Part 2, 2008, pp. 769–777. doi:10.4028/www.scientific.net/MSF.595-598.769

[14] Jouet, R. J., Carney, J. R., Granholm, R. H., Sandusky, H. W., and Warren, A. D., "Preparation and Reactivity Analysis of Novel Perfluoroalkyl Coated Aluminium Nanocomposites," *Materials Science and Technology*, Vol. 22, No. 4, April 2006, pp. 422–429. doi:10.1179/174328406X84003

[15] Struk, P. M., Ackerman, M., Nayagam, V., and Dietrich, D. L., "On Calculating Burning Rates During Fiber Supported Droplet Combustion," *Microgravity Science and Technology*, Vol. 11, No. 4, 1998, pp. 144–151.

[16] Williams, F. A., "Ignition and Burning of Single Liquid Droplets," *Proceedings of the Thirty Fifth Congress of the International Astronautical Federation*, AIAA, New York, 1984, pp. 547–553.

[17] Osborne, D. T., and Pantoya, M. L., "Effect of Aluminum Particle Size on the Thermal Degradation of Al/Teflon Mixtures," *Combustion Science and Technology*, Vol. 179, No. 8, 2007, pp. 1467–1480. doi:10.1080/00102200601182333

[18] Sarbak, Z., "Effect of Fluoride and Sodium Ions on Structural and Thermal Properties of *g*-AL2O3," *Crystal Research and Technology*, Vol. 32, No. 4, 1997, pp. 491–497. doi:10.1002/crat.2170320402

[19] Dean, S. W., and Pantoya, M. L., "The Influence of Alumina Passivation on Nano-Al/Teflon Reactions," *Thermochimica Acta*, Vol. 493, Nos. 1–2, 2009, pp. 109–110. doi:10.1016/j.tca.2009.03.018

[20] Pichon, S., Black, G., Chaumeix, N., Yahyaoui, M., Simmie, J. M., Curran, H. J., and Donohue, R., "The Combustion Chemistry of a Fuel Tracer: Measured Flame Speeds and Ignition Delays and a Detailed Chemical Kinetic Model for the Oxidation of Acetone," *Combustion and Flame*, Vol. 156, 2009, pp. 494–504. doi:10.1016/j.combustflame.2008.10.001

[21] Gan, Y., and Qiao, L., "Combustion Characteristics of Fuel Droplets with Addition of Nano and Micron Sized Aluminum Particles," *Combustion and Flame*, Vol. 158, No. 2, 2011, pp. 354–368. doi:10.1016/j.combustflame.2010.09.005

D. Talley
Editor-in-Chief